



Magnetic nitrogen-doped carbon derived from silk cocoon biomass: a promising and sustainable support for copper

Marzieh Tahmasbi¹ · Parisa Akbarzadeh¹ · Nadiya Koukabi¹

Received: 12 August 2021 / Accepted: 1 November 2021 / Published online: 26 November 2021
© The Author(s), under exclusive licence to Springer Nature B.V. 2021

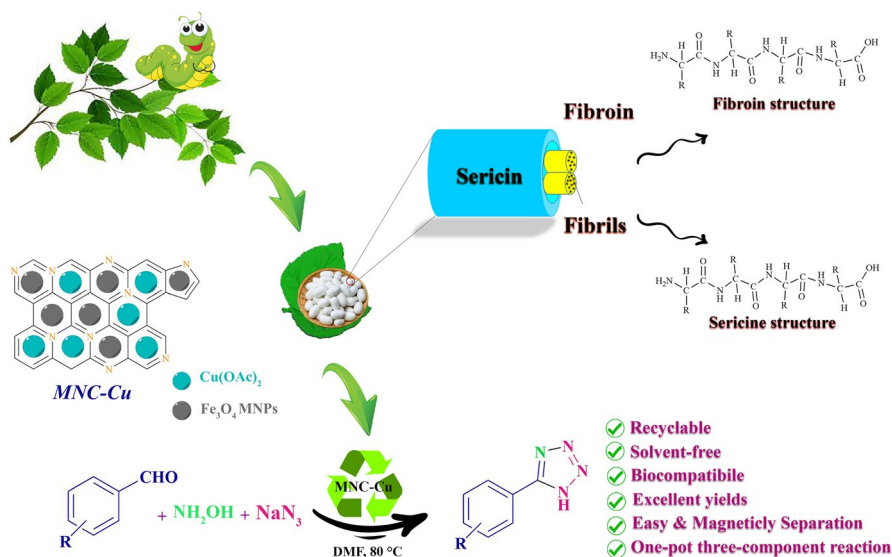
Abstract

In this study, a magnetic nitrogen-doped carbon-based copper (MNC-Cu) catalyst was fabricated so that natural silk cocoons undergo thermal processes and then activate by combining with Fe₃O₄ MNPs as a suitable substrate for placement copper metal. The efficiency of the generated catalyst in the synthesis of 5-substituted 1*H*-tetrazole derivatives was evaluated by the [3 + 2] cycloaddition reaction of aromatic aldehydes, azide ions, and hydroxylamines. FT-IR, FE-SEM, EDS, TEM, XRD, TGA, and VSM techniques have been adopted to identify and validate this heterogeneous catalyst. The observation from EDS, elemental mapping, XRD, and FT-IR analysis confirms the immobilization of Cu metals on the MNC surface and uniform distribution of species and then no aggregation occurs during functionalization. VSM results show the magnetic feature of fabricated catalyst, and based on the leaching test, the amount of catalyst leaching was negligible. Moreover, this reaction is a one-pot multicomponent reaction (MCRs) or more precisely a one-pot, three-component reaction, which is one of the advantages of this work. The fabricated catalyst shows high efficiency, good stability, and considerable reactivity in synthesizing 5-substituted 1*H*-tetrazole derivatives. So it can be seen that the fabricated magnetic catalyst is a useful and practical catalyst for synthesizing [3 + 2] cycloaddition reactions. Reusability and recyclability for five sequential runs without notable increase and reduction in activity are other advantages. In addition, the magnetic properties of this heterogeneous catalyst led to easy and quickly recovered and striking copper leaching.

✉ Nadiya Koukabi
n.koukabi@semnan.ac.ir

¹ Department of Chemistry, Semnan University, Semnan 35131-19111, Iran

Graphical abstract



Keywords Silk cocoon · Nitrogen-doped carbon · Copper nanoparticle · Tetrazole · Magnetic nanoparticles

Introduction

In recent decades, among the substances available to select suitable substrates for catalysts, heteroatom-doped carbon-based materials have attracted many researchers working in this field [1–3]. This interest is due to cost-effectiveness, low production costs, excellent thermal and chemical resistance, high surface-to-volume ratio, and the ability to control morphological structures properly [4]. The applications of this type of catalysts are not limited to specific fields and are broad and include various fields such as supercapacitors, adsorbents, lithium-ion batteries electrodes, and fuel cells [5–7]. These materials also can inspire the construction of many new catalysts in organic synthesis. The nitrogen-doped carbon with fortified heterogeneous sites and promoted porosity has gained special attention as support for new metals for catalytic designs [8].

Natural nitrogen-containing materials can be employed to manufacture nitrogen-based carbon catalysts [9, 10]. For example, the pyrolysis of nitrogen-rich biopolymers is one of the appropriate processes for synthesizing these materials [11–14]. Silk cocoons, a complex polymeric fibrous network, are used as carbon precursors to make nitrogen-doped carbon compounds that are available, inexpensive, and environmentally friendly following the principles of green chemistry and are suitable for this goal [15]. Silk cocoons contain fibroin and sericin,

providing carbon and nitrogen sources for making nitrogen-doped carbon compounds [16, 17]. At the temperature of 350 °C, the protein secondary structure, including β -sheet fibroin and α -helix sericin, can be turned into the sp^2 -hybridized structure or a hexagonal lattice structure of carbon atoms [18, 19]. This leads to an increase in the thermal stability of these compounds [20].

In this paper, we describe a new and economical method to provide nitrogen-rich carbon materials via a thermal carbonization route under a controlled temperature utilizing *Bombyx mori* silk cocoons as nitrogen and carbon sources and potassium hydroxide (KOH) as an activating agent. When potassium hydroxide is employed as an activating agent, potassium ions (K^+) combine with oxygen and carbon in silk cocoons to form potassium carbonate (K_2CO_3) during heat treatment. Eventually, pyrolysis of this combination produces potassium oxide (K_2O) and carbon dioxide (CO_2), which released carbon dioxide causes to form a porous structure. In addition, K_2O and residual K_2CO_3 were removed at the end of the NC substances' fabrication process by exposing them to the HCl solution and DI water [21, 22]. Creating a multilayer structure with a hierarchical porous structure saturated with uniformly doped nitrogen, easy removal of activating reagents, no demand for templates, and the considering of resulting carbon from silk cocoons as a sustainable source are important advantages of the thermal process of silkworm cocoons at a controlled temperature [23–25]. The main reason for the restricted application of nitrogen-doped carbon materials as a catalytic system in chemistry, notably organic chemistry, is the hard separation of these materials from the reaction medium after the end of the reaction. Thus, the manufacture of modified nitrogen-doped carbon materials and increasing efforts to improve these materials have been considered.

Fe_3O_4 MNPs is one of the materials utilized to develop this type of material, and due to its excellent advantages such as inexpensiveness, easy preparation, low toxicity, good thermal and chemical stability, it is broadly used in the modification of these structures [26–30]. A special advantage of using Fe_3O_4 MNPs is the magnetic separation of nitrogen-doped carbon materials, which as a green method, solves the problems related to filtration and centrifugation [31].

This paper is a sequence of former research on synthesizing heterogeneous and green catalysts made from silk cocoons and carbon-containing catalysts [32–34]. In this work, the fabrication of a new copper catalyst based on nitrogen-doped carbon materials and Fe_3O_4 MNPs as a substrate and its performance in synthesizing 5-substituted 1*H*-tetrazole derivatives has been investigated. Tetrazoles are among the most valuable nitrogen-rich heterocyclic compounds that have attracted much attention due to their charming features and comprehensive scope of utilization in diverse domains. Tetrazoles are broadly employed in numerous sciences and are chiefly applied in various chemistry branches, pharmaceuticals, and materials science [35, 36]. It can be declared that there are assorted approaches for the synthesis of this substance and its derivatives, including the reaction of primary amides with triazido-chlorosilane, aryl halides with potassium ferrocyanide, and oximes with diphenyl phosphorazidate or sodium azide. Despite this, the well-known and prevalent procedure of synthesizing tetrazole derivatives is through the [3 + 2] cycloaddition of azide ions and nitrile compounds by differing catalysts [37–41]. Herein we

use hydroxylamine, aromatic aldehydes, and sodium azide through a one-pot three-component reaction to achieve this goal.

Experimental

Preparation of NC

Similar to previous work [33], to achieve this, we heat silk cocoons in water and boil for 30 min, then rinse with distilled water, and dry for 12 h at 60 °C. For fabricate NC, two thermal processing stages are required, the first stage for 30 min at 500 °C with a heating rate of 5 °C/min and the second stage for 2 h at the same heating rate at 800 °C in a nitrogen atmosphere. The solid product obtained from the first stage is mixed with an activating reagent (KOH) with a ratio of 1:1 (w/w) by grinding and the mixture is ready for the carbonization second stage. In the second stage, the resulting mixture is heated in an alumina crucible under the mentioned conditions. The carbonized product was exposed to an HCl 5% solution for 12 h, rinsed with distilled water, and dried at 80 °C to synthesize NC [42].

Preparation of MNC

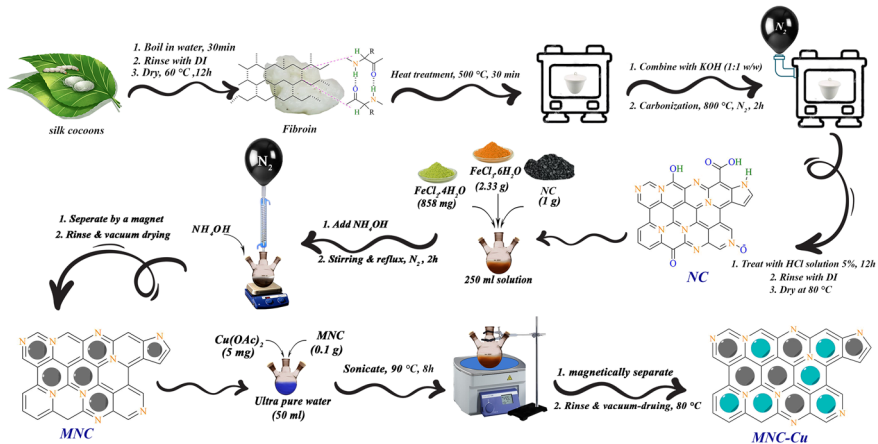
In this section, 1 g of NC was combined to 250 mL of an aqueous solution containing $\text{FeCl}_2 \cdot 4\text{H}_2\text{O}$ (0.858 g) and $\text{FeCl}_3 \cdot 6\text{H}_2\text{O}$ (2.33 g). Next, under reflux and stirring conditions, NH_4OH solution was combined with the mentioned mixture, and the reaction continued for 2 h under the N_2 atmosphere. An external magnet could separate the resulting black matter after rinsing and vacuum-drying.

Fabrication of MNC-Cu

In a round-bottom flask containing 50 mL deionized water, 0.1 g of MNC and 0.005 g of $\text{Cu}(\text{OAc})_2$ were added, and the mixture was sonicated and heated up at 90 °C for 8 h. Next, MNC-Cu was magnetically separated and rinsed with distilled water, followed by vacuum-drying at 80 °C (Scheme 1).

The general method for the synthesis of 5-substituted 1H-tetrazole derivatives

A combination of sodium azide (1.5 mmol), aromatic aldehyde (1 mmol), hydroxylamine (1.2 mmol), and MNC-Cu (0.26 mol% \cong 0.01 g) with 5 mL DMF was and stirred at 80 °C for the various time with heating (Table 2). The proceeding of the reaction was observed by thin-layer chromatography (TLC). After completing the reaction and cooling to ambient temperature, the fabricated catalyst was magnetically separated by an external magnet. After removing the catalyst, the remaining mixture's solvents were eliminated under reduced pressure and then dissolved in water. Afterward, HCl (15 mL, 2 N) was added to the aqueous solution to obtain a powder form of the tetrazole derivatives. The



Scheme 1 Procedure for preparation of MNC-Cu

precipitate was filtered and crystallized from a mixture of ethanol and water, and there was no need for further purification process via this route.

Results and discussion

Characterization of the catalyst

FT-IR analysis

FT-IR spectroscopy has been adopted to illustrate the diverse functional groups exhibited in the NC and MNC-Cu structures. Figure 1 shows that the NC and MNC-Cu structures exhibit a broad peak at 3425 cm^{-1} , which was attributed to the stretch vibrational mode of O–H and N–H. Furthermore, a peak that emerges at 1117 cm^{-1} was related to the C–O vibrational stretching mode. Also, peaks at 1680 cm^{-1} and 2312 cm^{-1} were assigned to the stretch vibrational mode of C=O and C=N, respectively [43]. The presence of the O–H, C=O, and C–OH bonds can be assigned to the reaction of carbon with potassium hydroxide during the activation process. FT-IR outcomes indicate that the amide group nitrogen in silk undergo carbonization and produce functional groups like N–H and C=N. The peaks at 783 cm^{-1} and 1570 cm^{-1} are related to aromatic C–H bending and aromatic C=C bending, respectively. Also, the peak at 2986 cm^{-1} corresponds to aromatic C–H stretching. In the MNC-Cu structure, we can recognize the strong peak at 580 cm^{-1} related to the Fe–O band, and the existing peak confirms that Fe₃O₄ MNPs were immobilized onto the structure.

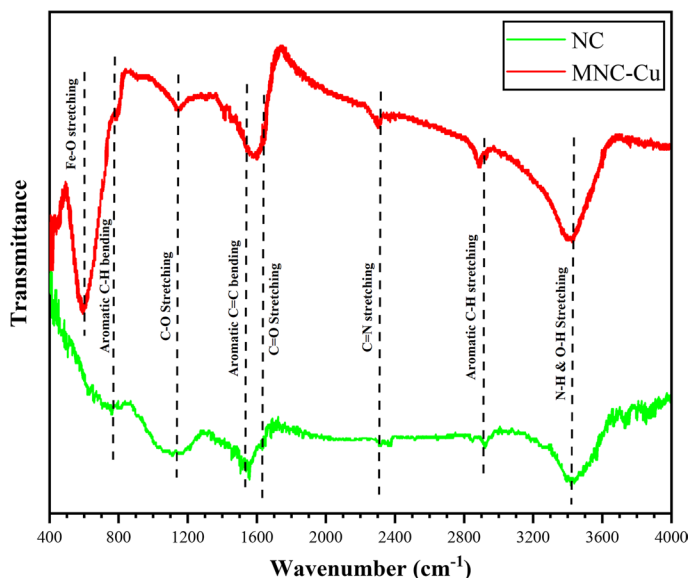


Fig. 1 FT-IR spectrum of MNC-Cu and NC

TGA analysis

TGA analysis was adopted under air atmosphere in the range of 25–800 °C at a heating rate of 10 °C/min to study the thermal stability of MNC-Cu and NC structures. The NC and MNC-Cu thermograms are shown in Fig. 2. According to the former papers, the silk cocoon decomposes at about 300 °C. The curve of manufactured NC and MNC-Cu structures indicates high thermal resistance.

EDX analysis

EDX spectrum rendered helpful data about the elements presented in the catalyst composition. As expected, it proved the presence of C, N, Fe, O, and Cu (Fig. 3). The copper quantity measured by EDX analysis was about 3.5 wt%.

SEM & TEM analysis

Level modifications of MNC and NC resulted in changes in morphology and structural features, which can be observed by SEM and TEM techniques. The information obtained from the SEM and TEM analysis are presented in Figs. 4 and 5, respectively. After the carbonization, the silk fibers turn into nitrogen-doped carbon fibers (NC), as shown in Figs. 4a, b and 5a. Numerous small pores randomly spread across the surfaces indicate that the fiber morphology improved

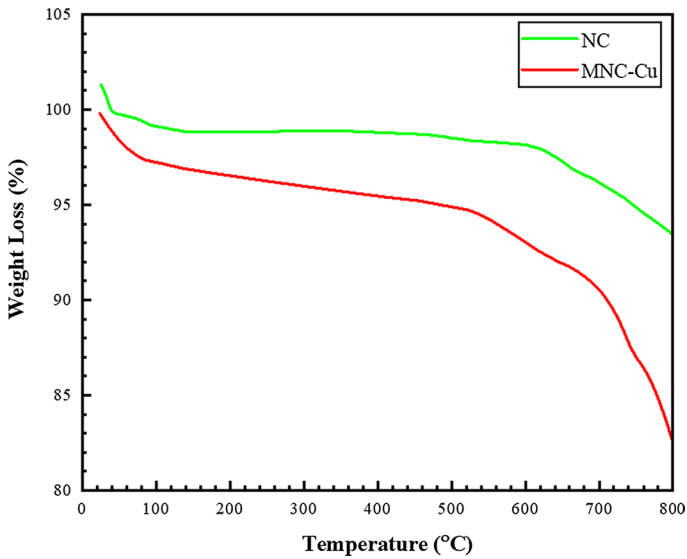


Fig. 2 TGA curves of NC and MNC-Cu

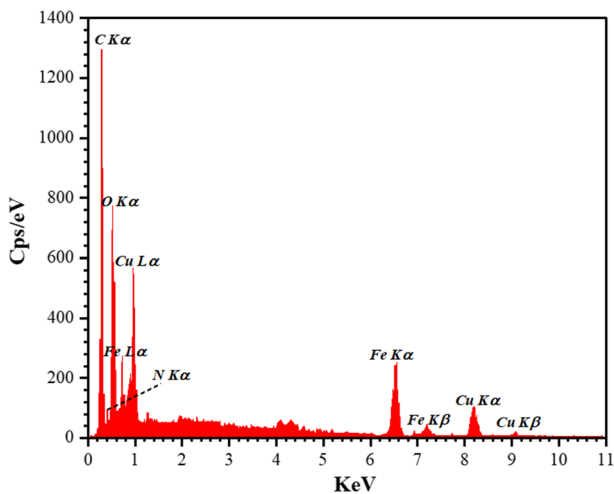


Fig. 3 EDX spectrum of MNC-Cu

after the high-temperature pyrolysis process. These small pores may be due to the release of CO_2 gas, and they leave the surface due to the carbonization reaction via KOH activation. The Cu and Fe_3O_4 nanostructures are evenly distributed on the prepared NC support surface, which can perceive from the SEM and TEM images presented in Figs. 4c–e and 5b.

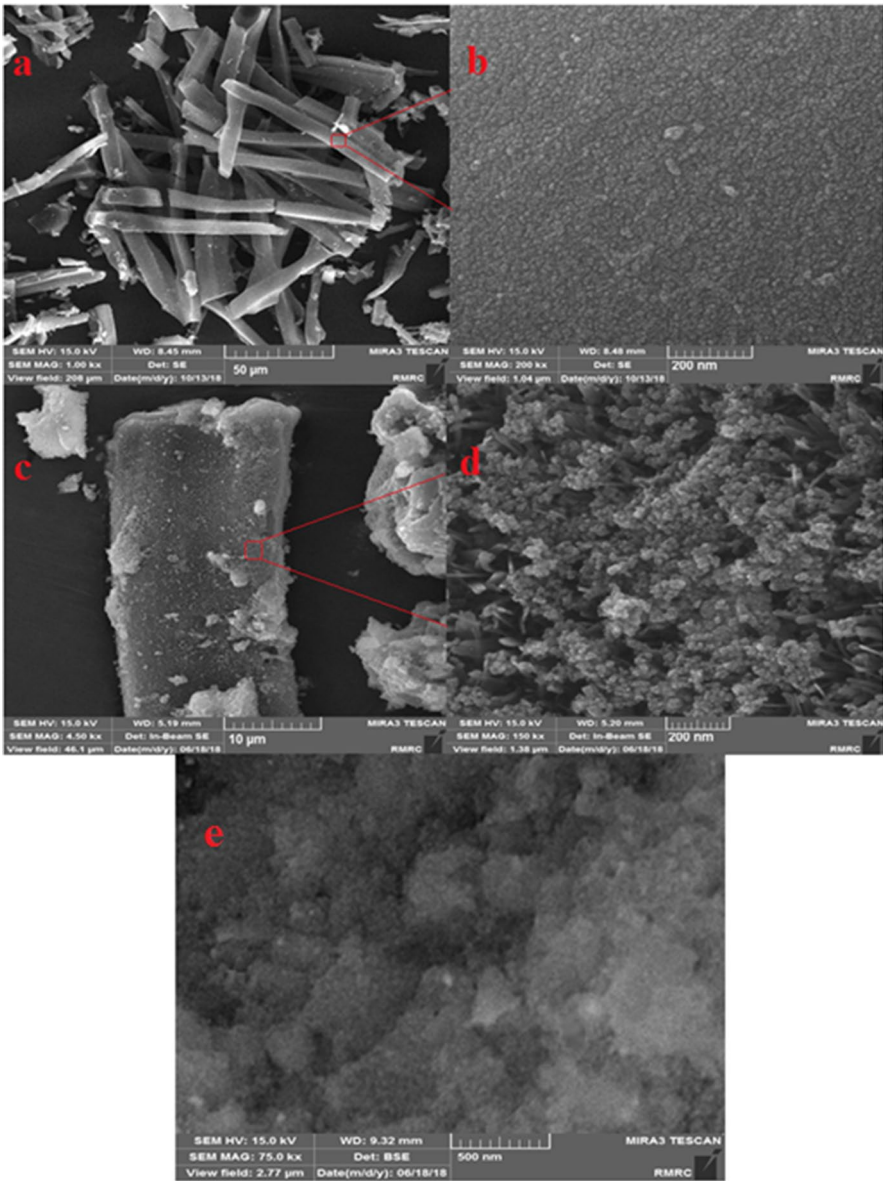


Fig. 4 SEM images of NC (**a**, **b**), MNC (**c**, **d**), and MNC-Cu (**e**)

XRD analysis

XRD analysis has been employed to evaluate the purity and crystal fabrication of the samples. The XRD patterns of NC and MNC are displayed in Fig. 6. The NC pattern exhibits peaks at 26.3° and 42.6° associated with planes (002) and (100) of

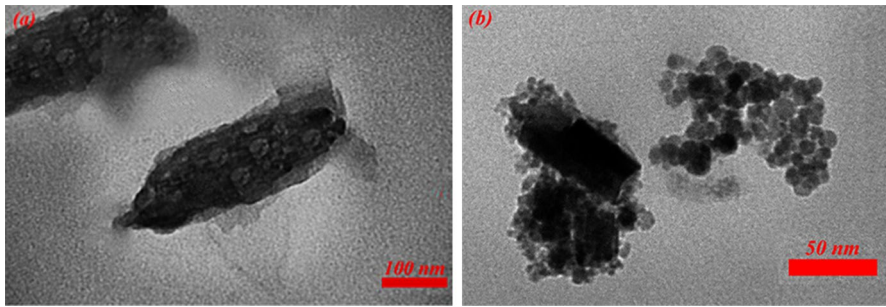


Fig. 5 TEM images of NC (a) and MNC-Cu (b)

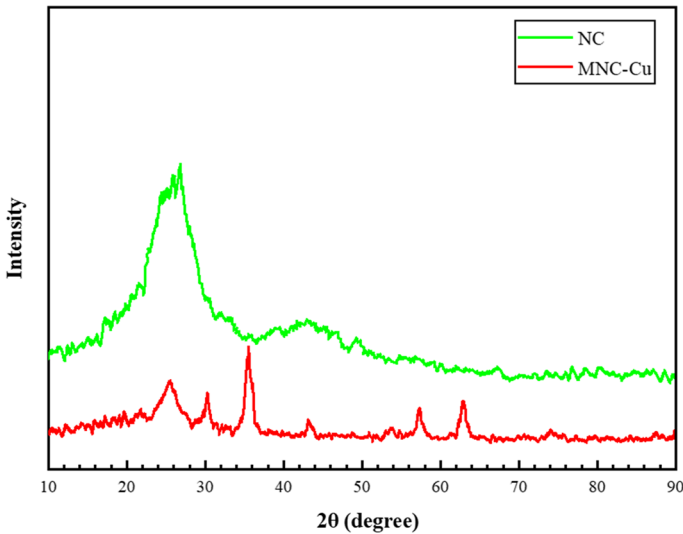


Fig. 6 The XRD patterns of NC and MNC

the hexagonal conjugate carbon structure, respectively [44]. The MNC pattern also shows specific peaks that are related to the structure of both NC and Fe_3O_4 . The six specified peaks are established at $2\theta = 30.86^\circ$, 36.26° , 43.15° , 53.81° , 57.19° , and 63.1° , corresponding to (220), (311), (400), (422), (511), and (440) planes of cubic magnetite with spinel structure, respectively (JCPDS 65–3107). Also, the peaks at 29.7° , 36.4° , 42.2° , 61.4° corresponding to (110), (111), (200), and (220) planes of Cu^{2+} which indicates the presence of it in the catalyst.

VSM analysis

VSM analysis was utilized at room temperature to determine the magnetic properties of the prepared MNC-Cu. The VSM analysis results in Fig. 7 show that the amount of saturation magnetization of MNC-Cu (15.33 emu/g) is lower than that of pure

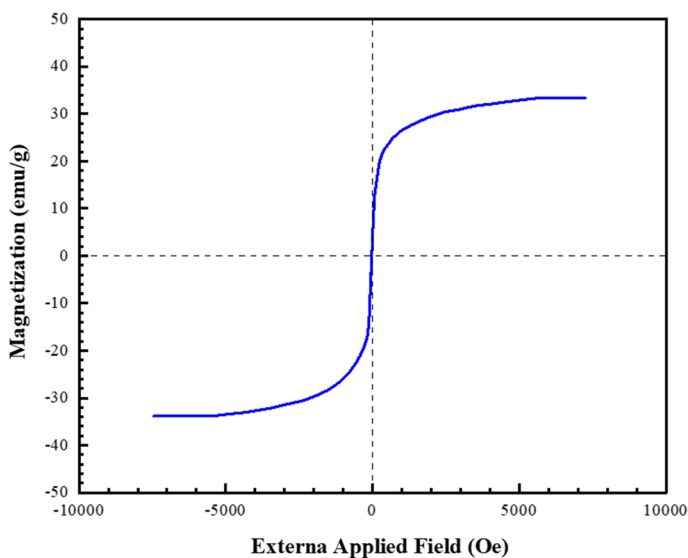


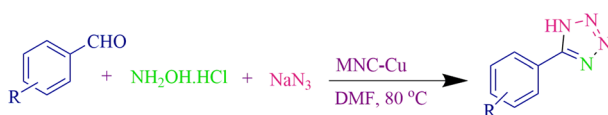
Fig. 7 VSM magnetization curve of MNC-Cu

Fe_3O_4 nanoparticles (61.60 emu/g). This information emphasizes the presence of non-magnetic substances such as NC and Cu nanoparticles in the catalyst. In any case, the catalyst can be swiftly eliminated from the reaction medium, applying a conventional method such as an external magnet.

Catalytic activity

One-pot synthesis of tetrazole derivatives was selected to evaluate the catalytic efficiency of MNC-Cu (Scheme 2).

To assess the optimal reaction conditions such as the quantity of sodium azide and catalyst, type of solvent, and temperature, we selected reaction of benzaldehyde, sodium azide, and hydroxylamine as a model reaction. Initially, the reaction was performed at several amounts of catalyst in DMF as solvent at 80 °C. The results showed that the amount of catalyst required for the optimal condition was 0.26 mol%, which revealed high and effective performance in 2.5 h. However, more use of the optimized catalyst amount does not significantly affect the final reaction efficiency, and it means that it does not reduce the reaction time or increase the efficiency of the product. Also, using a smaller amount of catalyst will prolong the reaction time and reduce overall efficiency.



Scheme 2 Tetrazoles catalyzed by MNC-Cu nanocomposite

When the model reaction was performed without catalyst, the product was generated with a meager yield (Table 1, entries 1–6). In order to characterize the optimum temperature, various temperatures were examined for the model reaction, and it was realized that the 80 °C temperature could be more efficient (Table 1, entries 3,7,8,9). Also, NaN_3 quantity could alter the reaction efficiency (Table 1, entries 10–11). 1.5 mmol of NaN_3 was determined as an optimum amount for the model reaction. After optimizing the mass of the catalyst and temperature, the solvents' optimization was examined, and for this aim, various solvents were applied to achieve maximum performance in the model reaction. At first, the reaction was carried out under solvent-free conditions, but DMF could give the best outcome (Table 1, entries 3, 12–16). Consequently, the optimized reaction condition is provided in entry 3 at 80 °C with 0.26 mol% MNC-Cu and 1.5 mmol of NaN_3 in DMF solvent.

Indeed to blank control test and evaluate the autocatalytic effect of Fe metal, the $\text{Fe}_3\text{O}_4\text{-NC}$ substance was used in the model reaction, and the results show that the reaction progressed with the 54% yield at 4.5 h. In comparison, the reaction model proceeded with the 95% yield at 2.5 h in the presence of $\text{Fe}_3\text{O}_4\text{-NC-Cu}$ substance.

Various aldehydes comprising both electron-donating and electron-withdrawing groups were engaged in this reaction, as shown in Table 2. All precursors provided the desired products with excellent yields (Table 2). Nevertheless, due to the reduced electrophilic properties of the carbonyl function, the reaction with electron-donating aldehydes required a longer time (Table 2, entries 6–11). Further, steric effects could be seen in this process. For example, compared with 4chlorobenzaldehyde, the reaction

Table 1 Optimization of reaction condition for synthesis of 5-substituted 1*H*-tetrazoles ^a

Entry	Catalyst amount (mol %)	NaN_3 (mmol)	Temperature (°C)	Solvent	Time (h)	Yield (%) ^b
1	–	1.5	80	DMF	6	Trace
2	0.20	1.5	80	DMF	2:30	70
3	0.26	1.5	80	DMF	2:30	95
4	0.50	1.5	80	DMF	2:30	96
5	0.26 ^c	1.5	80	DMF	3	trace
6	0.26 ^d	1.5	80	DMF	3	30
7	0.26	1.5	R.T	DMF	3	Trace
8	0.26	1.5	50	DMF	2:30	72
9	0.26	1.5	110	DMF	2:30	95
10	0.26	1	80	DMF	2:30	74
11	0.26	2	80	DMF	2:30	95
12	0.26	1.5	110	–	2:30	Trace
13	0.26	1.5	80	H_2O	2:30	60
14	0.26	1.5	80	DMSO	2:30	45
15	0.26	1.5	Reflux	EtOH	2:30	50
16	0.26	1.5	Reflux	Toluene	2:30	55

^a Reaction conditions: aromatic aldehyde (1 mmol), hydroxylamine (1.2 mmol), sodium azide, MNC-Cu catalyst (0.26 mol%)

^b Isolated yield

Table 2 Synthesis of diverse tetrazoles catalyzed by MNC-Cu nanocomposite ^a

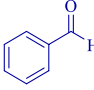
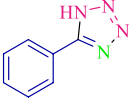
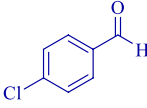
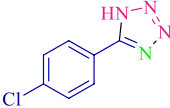
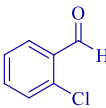
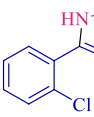
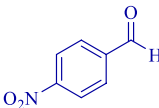
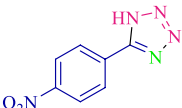
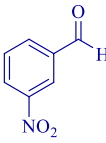
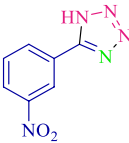
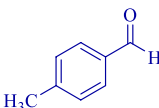
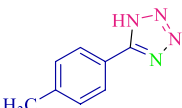
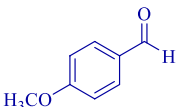
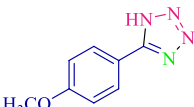
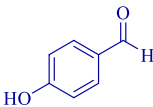
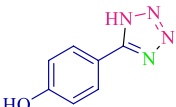
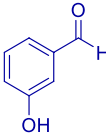

Entry	Reactant	Time (h)	Product	Yield (%) ^b	M.p. (°C) [ref.]
1		2:30	 2a _{2a}	95	213–215 [37]
2		3:10	 2b _{2b}	93	181–183 [37]
3		4:00	 2c _{2c}	85	176–177 [38]
4		2:30	 2d _{2d}	95	215–218 [37]
5		2:50	 2e _{2e}	90	156–158 [38]
6		3:40	 2f _{2f}	88	250–251 [37]
7		3:40	 2g _{2g}	82	230–233 [37]
8		4:15	 2h _{2h}	90	234–236 [37]
9		4:35	 2i _{2i}	91	243–246 [37]

Table 2 (continued)

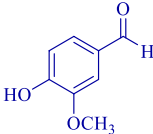
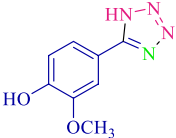
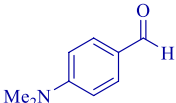
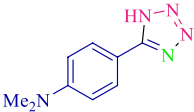
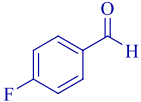
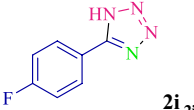
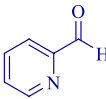
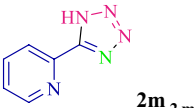
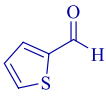
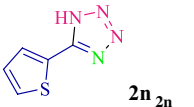
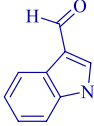
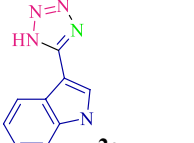
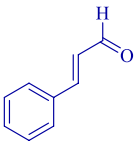
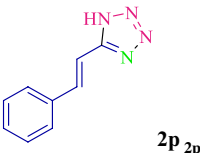
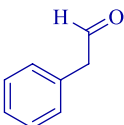
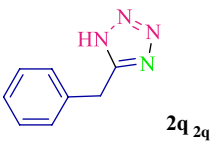
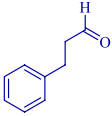
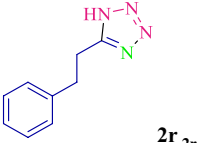
Entry	Reactant	Time (h)	Product	Yield (%) ^b	M.p. (°C) [ref.]
10		3:40	 2j _{2j}	89	220–223 [38]
11		4:45	 2k _{2k}	85	134–135 [38]
12		3:10	 2i _{2i}	92	203–206 [38]
13		3:15	 2m _{2m}	90	209–212 [37]
14		2:50	 2n _{2n}	90	207–208 [38]
15		4:50	 2o _{2o}	82	160–163 [37]
16		4:50	 2p _{2p}	80	155–156 [38]
17		6:00	 2q _{2q}	82	120–122 [37]
18		6:30	 2r _{2r}	80	103–105 [37]

Table 2 (continued)

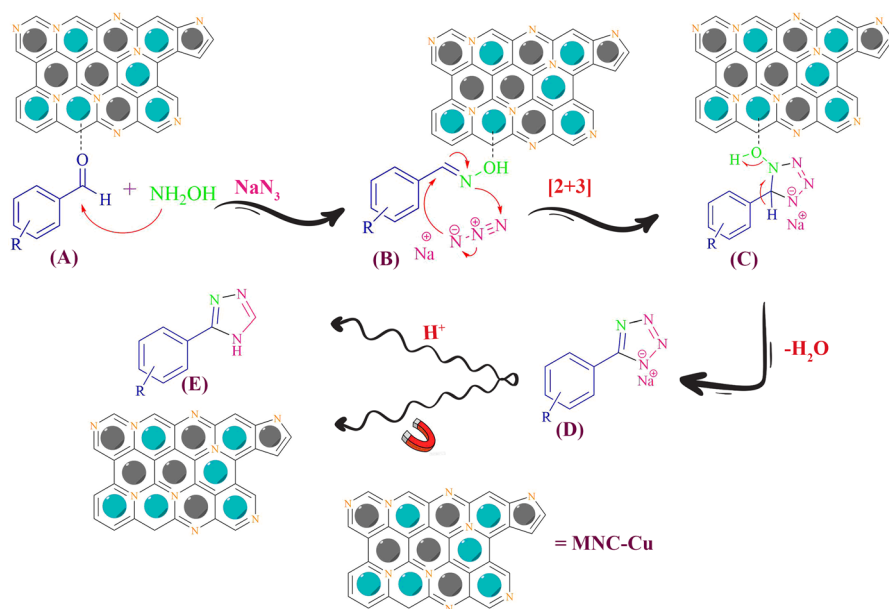
^a Reaction conditions: aromatic aldehyde (1 mmol), hydroxylamine (1.2 mmol), NaN_3 (1.5 mmol), MNC-Cu (0.26 mol%), DMF (3 mL), 80 °C

^b Isolated yield

with 2-chlorobenzaldehyde resulted in a lower yield within a longer time (Table 2, entries 2,3). The reaction with heteroaromatic aldehydes containing 3-indole carboxaldehyde, 2-pyridine carboxaldehyde, and 2-thiophene carboxaldehyde produced related products in the excellent outcome (Table 2, entries 13–15). The performance of MNC-Cu was outstanding in the synthesis of aliphatic tetrazole derivatives (Table 2, entries 17–18). These results proved that for preparing tetrazole derivatives, the MNC-Cu is a highly active heterogeneous catalyst.

Reaction mechanism

An acceptable mechanism is suggested in Scheme 3. At first, the carbonyl function of compound (A) is activated by the catalyst, and then the nitrogen atom of hydroxylamine attacks the activated carbonyl to create the oxime compound (B). At second, the oxygen atom of the oxime function is coordinated with the catalyst to set the stage for [2+3] cycloaddition. The cycloaddition reaction between the oxime compound (B) and the azide ion produces compound (C), which can undergo water elimination to afford tetrazole salt (D). Finally, upon treatment of HCl with the salt, tetrazole compound (E) is formed.



Scheme 3 A possible mechanism for the synthesis of tetrazoles utilizing MNC-Cu

Catalytic activity comparison of MNC-Cu with the recently reported catalysts for the synthesis of tetrazole derivatives

A comparative analysis is presented in Table 3 in order to show the high performance of MNC-Cu. The result of using our catalyst proved that the MNC-Cu is beneficial in this process, and other catalysts have several drawbacks, including lengthy reaction period (Table 3, entrance, 1, 2, 5, 6), and high temperature (Table 3, entries 1, 2, 3, 4, 5).

Reusability of the catalyst

One of the significant and influential factors for economic and commercial applications is reusing the catalyst. For this purpose, after the first cycle, the catalyst is removed by an easy and fast method with an external magnet. In the next step, the catalyst was rinsed with ethanol as the solvent and then was dried in a vacuum at 80 °C. Then, the separated catalyst was transferred to a reaction vessel for reuse. Consequently, the reusability of this catalyst was evaluated in five consecutive cycles, as shown in Fig. 8. According to the information given in Fig. 8, it can be seen that the reaction did not show a significant decrease during the five evaluated cycles. Besides, the EDX analysis was applied to investigate alterations in the elemental composition of MNC-Cu. The EDX analysis pattern in Fig. 9, which was examined for five cycles, shows a small amount of copper remaining after this time.

For identifying the leaching of copper from the catalyst, the catalyst was separated from the reaction vessel after 50 min, and the residual combined was retained to continue the reaction under optimized conditions. Based on Fig. 10, after 180 min passed, a scanty increase was observed. Results demonstrated the real heterogeneous nature of the catalyst.

Table 3 Comparison of MNC-Cu with other recently reported catalysts for preparing 5-phenyl-1H-tetrazole

Entry	Catalyst	Condition	Time (h)	Yield (%)	Reference
1	Cu-MCM-41	DMF, 140 °C	12	90	[38]
2	Cu(OAc) ₂	DMF, 120 °C	12	96	[39]
3	P ₂ O ₅	DMF, Reflux	4	90	[45]
4	(NH ₄) ₄ Ce(SO ₄) ₄ ·2H ₂ O	DMF, Reflux	5	72	[46]
5	Bi(OTf) ₃	DMF, 120 °C	24	87	[40]
6	Nano-Cu ₂ O-MFR ^a	DMF, 100 °C	8	92	[41]
7	Cu(OAc) ₂ ^b	DMF, 120 °C	12	98	[47]
8	InCl ₃ ^b	DMF, 120 °C	15	92	[48]
9	MNC-Cu	DMF, 80 °C	2.5	95	This work

^a Melamine–formaldehyde resin

^b The substrate is benzaldoxime

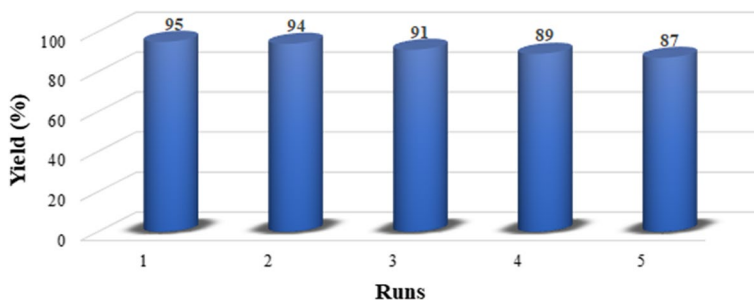


Fig. 8 Recycling experiment of the MNC-Cu nanocomposite

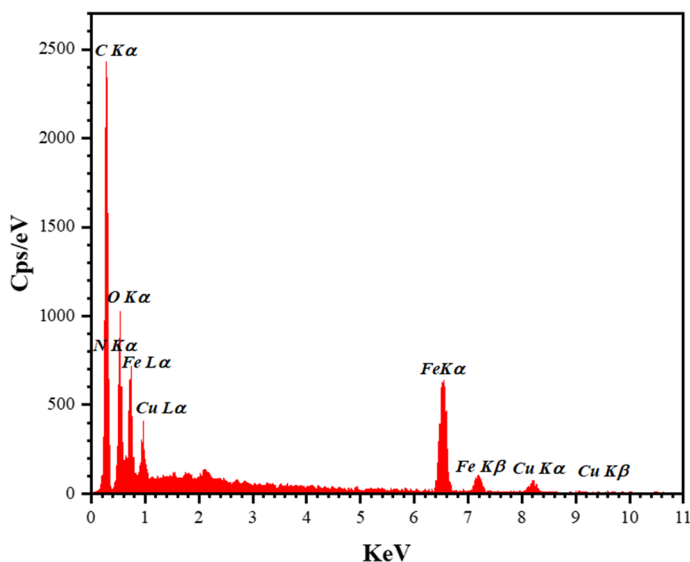


Fig. 9 EDX spectra of the recovered MNC-Cu after being reused five times

Conclusion

This work focuses on biodegradable substrates such as biopolymer silk fibroin scaffolds (SF) as a template for material support, metal anchoring, and its application in organic reactions. Briefly, the nitrogen-doped carbon catalyst and its combination with magnetic Fe_3O_4 nanoparticles were evaluated as a suitable substrate for copper anchoring. To achieve this goal, we utilized silk cocoons during two thermal processing steps, and then after several stages, we succeeded in fabricating MNC-Cu and applying it as a catalyst in the synthesis of tetrazole derivatives. Some experience data confirmed the resulting catalyst, such as FT-IR, TGA, EDX, TEM, XRD, SEM, and VSM. These studies demonstrated that

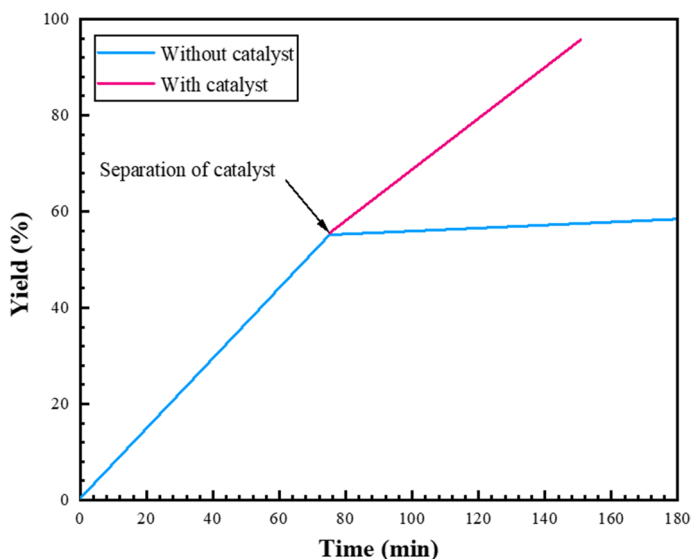


Fig. 10 Leaching experiment of MNC-Cu

immobilizing copper metal onto magnetic nitrogen-doped carbon and manufacturing MNC-Cu had a positive effect such as easy and magnetic separation, biodegradation, and excellent catalytic performance in the synthesis of 5-substituted 1*H*-tetrazole derivatives. High efficiency, good thermal stability, and considerable reactivity during continuous cycles are other features of designed MNC-Cu as a candidate for use in one-pot multicomponent reactions. In addition to the mentioned advantages, the ability to use the catalyst five times without significant change and reduction in its performance and following the principles and bases of green chemistry both in the catalyst manufacturing and application stage can be counted among the advantages of this catalyst. This paper can inspire future work in this field and can cause creative ideas for different topics.

Supplementary Information The online version contains supplementary material available at <https://doi.org/10.1007/s11164-021-04623-3>.

Acknowledgements The authors sincerely acknowledge the Research Council of Semnan University for supporting this work.

Funding Semnan University, Grant Recipient: Dr. Nadiya Koukabi, Associated Professor.

Availability of data and material My manuscript has data included as supplementary electronic material.

Declarations

Conflict of interest All authors are aware of the submission and agree to its publication and have no conflict of interest.

References

1. S. Gopi, K. Giribabu, M. Kathiresan, *ACS Omega* **3**, 6251 (2018)
2. B. Karimi, H. Barzegar, H. Vali, *Chem. Commun.* **54**, 7155 (2018)
3. B. Sakintuna, Y. Yürüm, *Ind. Eng. Chem. Res.* **44**, 2893 (2005)
4. F. Bai, Y. Xia, B. Chen, H. Su, Y. Zhu, *Carbon N. Y.* **79**, 213 (2014)
5. Z. Lan, Y. Fang, Y. Zhang, X. Wang, *Angew. Chemie* **130**, 479 (2018)
6. J. Lee, J. Kim, T. Hyeon, *Adv. Mater.* **18**, 2073 (2006)
7. M.J. Bojdys, J. Jeromenok, A. Thomas, M. Antonietti, *Adv. Mater.* **22**, 2202 (2010)
8. R. Wang, K. Wang, Z. Wang, H. Song, H. Wang, S. Ji, *J. Power Sources* **297**, 295 (2015)
9. X.-H. Li, M. Antonietti, *Chem. Soc. Rev.* **42**, 6593 (2013)
10. X. Chen, Y.S. Jun, *Chem. Mater* **21**, 150 (2009)
11. S.Y. Cho, Y.S. Yun, S. Lee, D. Jang, K.-Y. Park, J.K. Kim, B.H. Kim, K. Kang, D.L. Kaplan, H.-J. Jin, *Nat. Commun.* **6**, 1 (2015)
12. P. Zhang, Y. Gong, H. Li, Z. Chen, Y. Wang, *Nat. Commun.* **4**, 1 (2013)
13. P.E. Ingham, *J. Appl. Polym. Sci.* **15**, 3025 (1971)
14. M.-M. Titirici, M. Antonietti, *Chem. Soc. Rev.* **39**, 103 (2010)
15. H.-S. Kim, S.H. Yoon, S.-M. Kwon, H.-J. Jin, *Biomacromol* **10**, 82 (2009)
16. R. Nazarov, H.-J. Jin, D.L. Kaplan, *Biomacromol* **5**, 718 (2004)
17. C. Fu, Z. Shao, and V. Fritz, *Chem. Commun.* **45**, 6515 (2009)
18. H.-W. Liang, S. Brüller, R. Dong, J. Zhang, X. Feng, K. Müllen, *Nat. Commun.* **6**, 1 (2015)
19. H.H. Kim, M.K. Kim, K.H. Lee, Y.H. Park, I.C. Um, *Int. J. Biol. Macromol.* **79**, 943 (2015)
20. D. Lardizábal-G, Y. Verde-Gómez, I. Alonso-Lemus, A. Aguilar-Elguezabal, *Int. J. Hydrogen Energy* **40**, 17300 (2015)
21. Z. Heidarinejad, M.H. Dehghani, M. Heidari, G. Javedan, I. Ali, M. Sillanpää, *Environ. Chem. Lett.* **18**, 393 (2020)
22. H. Tounsadi, A. Khalidi, M. Farnane, M. Abdennouri, N. Barka, *Process Saf. Environ. Prot.* **102**, 710 (2016)
23. Z. Hezarkhani, A. Shaabani, *Appl. Organomet. Chem.* **31**, e3624 (2017)
24. Y. Zhu, W. Sun, J. Luo, W. Chen, T. Cao, L. Zheng, J. Dong, J. Zhang, M. Zhang, Y. Han, *Nat. Commun.* **9**, 1 (2018)
25. J. Wang, S. Kaskel, *J. Mater. Chem.* **22**, 23710 (2012)
26. M. Ma, Q. Zhang, D. Yin, J. Dou, H. Zhang, H. Xu, *Catal. Commun.* **17**, 168 (2012)
27. M.A. Bodaghifard, *J. Organomet. Chem.* **886**, 57 (2019)
28. Q. Du, W. Zhang, H. Ma, J. Zheng, B. Zhou, Y. Li, *Tetrahedron* **68**, 3577 (2012)
29. A. Marandi, N. Koukabi, *Colloids Surf. A Physicochem. Eng. Asp.* **621**, 126597 (2021)
30. A. Marandi, E. Nasiri, N. Koukabi, F. Seidi, *Int. J. Biol. Macromol.* **190**, 61 (2021)
31. C.W. Lim, I.S. Lee, *Nano Today* **5**, 412 (2010)
32. P. Akbarzadeh, N. Koukabi, *Appl. Organomet. Chem.* **34**, e5395 (2020)
33. P. Akbarzadeh, N. Koukabi, *Appl. Organomet. Chem.* **35**, e6039 (2021)
34. A. Marandi, N. Koukabi, M.A. Zolfigol, *Res. Chem. Intermed.* **47**, 3145 (2021)
35. P. Akbarzadeh, N. Koukabi, E. Kolvari, *Mol. Divers.* **24**(2), 319 (2019)
36. P. Akbarzadeh, N. Koukabi, E. Kolvari, *Res. Chem. Intermed.* **45**, 1009 (2019)
37. M. Esmailpour, A.R. Sardarian, H. Firouzabadi, *Appl. Organomet. Chem.* **32**, e4300 (2018)
38. M. Abdollahi-Alibeik, A. Moaddeli, *New J. Chem.* **39**, 2116 (2015)
39. M.M. Heravi, A. Fazeli, H.A. Oskooie, Y.S. Beheshtiha, H. Valizadeh, *Synlett* **23**, 2927 (2012)
40. M. Sridhar, K.K.R. Mallu, R. Jillella, K.R. Godala, C.R. Beeram, N. Chinthala, *Synthesis (Stuttg.)* **45**, 507 (2013)
41. S. Behrouz, *J. Saudi Chem. Soc.* **21**, 220 (2017)
42. J. Sun, Z. Zhang, J. Ji, M. Dou, F. Wang, *Appl. Surf. Sci.* **405**, 372 (2017)
43. T. Altun, E. Pehlivan, *Food Chem.* **132**, 693 (2012)
44. V. Sahu, S. Grover, B. Tulachan, M. Sharma, G. Srivastava, M. Roy, M. Saxena, N. Sethy, K. Bhargava, D. Philip, *Electrochim. Acta* **160**, 244 (2015)
45. K.M. Khan, I. Fatima, S.M. Saad, M. Taha, W. Voelter, *Tetrahedron Lett.* **57**, 523 (2016)

46. B. Mitra, S. Mukherjee, G.C. Pariyar, P. Ghosh, *Tetrahedron Lett.* **59**, 1385 (2018)
47. U.B. Patil, K.R. Kumthekar, J.M. Nagarkar, *Tetrahedron Lett.* **53**, 3706 (2012)
48. S.D. Guggilapu, S.K. Prajapati, A. Nagarsenkar, K.K. Gupta, B.N. Babu, *Synlett* **27**, 1241 (2016)

Publisher's Note Springer Nature remains neutral with regard to jurisdictional claims in published maps and institutional affiliations.